Vol 16 No 8, August 2007
1009-1963/2007/16(08)/2229-08

Chinese Physics

© 2007 Chin. Phys. Soc.
and IOP Publishing Ltd

# Entanglement in an anisotropic spin-1 Heisenberg chain*

Zhu Yan(朱 燕), Zhu Shi-Qun(朱士群)†, and Hao Xiang (郝 翔)

*School of Physical Science and Technology, Suzhou University, Suzhou* 215006, *China*

(Received 15 December 2006; revised manuscript received 16 January 2007)

The entanglement in an anisotropic spin-1 Heisenberg chain with a uniform magnetic field is investigated. The ground-state entanglement will undergo two different kinds of transitions when the anisotropy $\Delta$ and the amplitude of the magnetic field $B$ are varied. The thermal entanglement of the nearest neighbour always declines when $B$ increases no matter what the value of the anisotropy is. It is very interesting to note that the entanglement of the next-nearest neighbour can increase to a maximum at a certain magnetic field. Regardless of the boundary condition, the nearest-neighbour entanglement always decreases and approaches to a constant value when the size of the system is very large. The constant value of open boundary condition is much larger than that of periodic boundary condition.

**Keywords:** entanglement, Heisenberg chain, open boundary condition, periodic boundary condition
**PACC:** 0365, 7510J

## 1. Introduction

As a fundamental kind of quantum resource, entanglement plays an important role in quantum computation and quantum communication.[1−6] Especially in recent years, much attention has been paid to the study of the entanglement properties of two-level solid state systems.[7−12] It is theoretically shown that the quantum computation[13−15] and perfect quantum state transfer[16] can be realized via the entanglement in a solid-state system. In condensed matter systems, spin-1/2 models[7,17,18] are considered to as natural candidates of qubit systems where various forms of entanglement exist at low temperatures. Using the spin-1/2 chain to implement quantum teleportation was discussed.[19] Such quantum systems includes finite spin clusters[20−23] and infinite spin systems[17,24−28] where quantum phase transition can be detected at the ground state.[27,28] The entanglement in any thermal equilibrium state has also been widely studied.[7,17,29,30] The effects of the inhomogeneous magnetic field[18] and the frustrate interaction[31] on the entanglement in spin-1/2 Heisenberg models have been considered. To detect the entanglement experimentally, the witness, which can provide a sufficient condition for the presence of the entanglement[27,32,33] has been used. However, many real solid state systems[7,34−36] have complicated energy levels that are always modelled by spin-$s$ quantum systems $\left(s > \frac{1}{2}\right)$. Because of the inherent structures, high-dimensional quantum systems are clearly different from two-dimensional ones. For spin-1 Heisenberg quantum systems, their phase diagrams, magnetic and thermal properties are unique,[34] It is necessary to analyse their entanglement properties, which is helpful to the high-dimensional quantum computation and quantum communication. Meanwhile, the negativity[21,37] can also been used to conveniently evaluate the entanglement of spin-1 Heisenberg chain.

In this paper, the general form of an anisotropic spin-1 Heisenberg chain in a uniform magnetic field is investigated. In Section 2, two-spin ground state is derived. With the variation of the magnetic field $B$, the transitions of the entanglement are discussed. The effects of the thermal temperature $T$ and the anisotropy $\Delta$ on the entanglement are studied in Section 3. For a many-spin Heisenberg chain, the nearest-neighbour entanglement and the next-nearest-neighbour entanglement are numerically calculated when the magnetic field is varied. In Section 4, the effects of the boundary

*Project supported by the Specialized Research Fund for the Doctoral Program of Higher Education of China (Grant No 20050285002).

†Corresponding author. E-mail: szhu@suda.edu.cn

conditions and the size of the system are presented. A discussion is given in Section 5.

## 2. Entanglement transitions of ground state

Since the ground state is very important in many quantum systems, it is necessary to investigate the ground-state entanglement. The general condition of an anisotropic spin-1 Heisenberg chain with the number of spins $L$ is considered. The Hamiltonian $H$ in uniform magnetic field $B$ can be described by

$$H=\sum_{i=1}^{L}\frac{J}{2}(S_i^+S_{i+1}^- + S_i^-S_{i+1}^+ + 2\Delta S_i^zS_{i+1}^z) + BS_i^z, \tag{1}$$

where $S_i^{\pm}$ are the lifting and lowering operators for the $i$th spin and $S_i^z$ is the $z$-component of spin operator. For convenience, $|1\rangle$, $|0\rangle$ and $|-1\rangle$ are assumed to be the eigenstates of $S_i^z$ with corresponding eigenvalues of $1, 0$, and $-1$ respectively. The parameter $B$ is the amplitude of the magnetic field along the $z$-axis, $J$ is the exchange interaction and $\Delta$ is an anisotropy coefficient which is less than one. The antiferromagnetic and ferromagnetic cases correspond to $J>0$ and $J<0$ respectively. In order to enter into the entanglement between any two spins, the negativity[21,37] is introduced as follows:

$$N(\rho)=|\sum_i \mu_i|, \tag{2}$$

where $\mu_i$ is the negativity eigenvalue of $\rho^{T_1}$, which is the partial transpose of the matrix $\rho$. Without losing the generality, the simplest case of $L=2$ is considered. In the space expanded by $\{|1\rangle|1\rangle,\ |1\rangle|0\rangle,\ |1\rangle|-1\rangle,\ |0\rangle|1\rangle,\ |0\rangle|0\rangle,\ |0\rangle|-1\rangle,\ |-1\rangle|1\rangle,\ |-1\rangle|0\rangle,\ |-1\rangle|-1\rangle\}$, the matrix expression of the Hamiltonian $H$ can be given by

$$H=\begin{pmatrix}
2B+2J\Delta & 0 & 0 & 0 & 0 & 0 & 0 & 0 & 0\\
0 & B & 0 & 2J & 2J & 0 & 0 & 0 & 0\\
0 & 0 & -2J\Delta & 0 & 0 & 0 & 0 & 0 & 0\\
0 & 2J & 0 & B & 0 & 0 & 0 & 0 & 0\\
0 & 0 & 2J & 0 & 0 & 0 & 2J & 0 & 0\\
0 & 0 & 0 & 0 & 0 & -B & 0 & 2J & 0\\
0 & 0 & 0 & 0 & 2J & 0 & 2J\Delta & 0 & 0\\
0 & 0 & 0 & 0 & 0 & 2J & 0 & -B & 0\\
0 & 0 & 0 & 0 & 0 & 0 & 0 & 0 & 2B+2J\Delta
\end{pmatrix}. \tag{3}$$

Because the total spin $S^z=\sum_i S_i^z$ is conserved in this model, i.e. $[H,S^z]=0$, the eigenstates $|\psi_i\rangle$ and corresponding eigenvalues $E_i$ can be expressed as

$$\begin{aligned}
E_1 &= 2B+2J\Delta, & |\Psi_1\rangle &= |1\rangle|1\rangle,\\
E_2 &= 2J+B, & |\Psi_2\rangle &= \frac{1}{\sqrt{2}}(|1\rangle|0\rangle+|0\rangle|1\rangle),\\
E_3 &= -2J+B, & |\Psi_3\rangle &= \frac{1}{\sqrt{2}}(|1\rangle|0\rangle-|0\rangle|1\rangle),\\
E_4 &= 2J-B, & |\Psi_4\rangle &= \frac{1}{\sqrt{2}}(|0\rangle|-1\rangle+|-1\rangle|0\rangle),\\
E_5 &= -2J-B, & |\Psi_5\rangle &= \frac{1}{\sqrt{2}}(|0\rangle|-1\rangle-|-1\rangle|0\rangle),\\
E_6 &= -2J\Delta, & |\Psi_6\rangle &= \frac{1}{\sqrt{2}}(|1\rangle|-1\rangle-|-1\rangle|1\rangle),\\
E_7 &= 4JX_+, & |\Psi_7\rangle &= a_+(|1\rangle|-1\rangle+|-1\rangle|1\rangle)+b_+|0\rangle|0\rangle,\\
E_8 &= 4JX_-, & |\Psi_8\rangle &= a_-(|1\rangle|-1\rangle+|-1\rangle|1\rangle)+b_-|0\rangle|0\rangle,\\
E_9 &= -2B+2J\Delta, & |\Psi_9\rangle &= |-1\rangle|-1\rangle,
\end{aligned} \tag{4}$$

where the parameters $X_\pm = \frac{1}{4}(-\Delta \pm \sqrt{\Delta^2+8})$, $b_\pm = 1/\sqrt{1+2X_\pm^2}$, and $a_\pm = b_\pm X_\pm$. From Eqs.(2)–(4), the negativity $N(\rho)$ of the ground-state entanglement for two spins can be obtained.

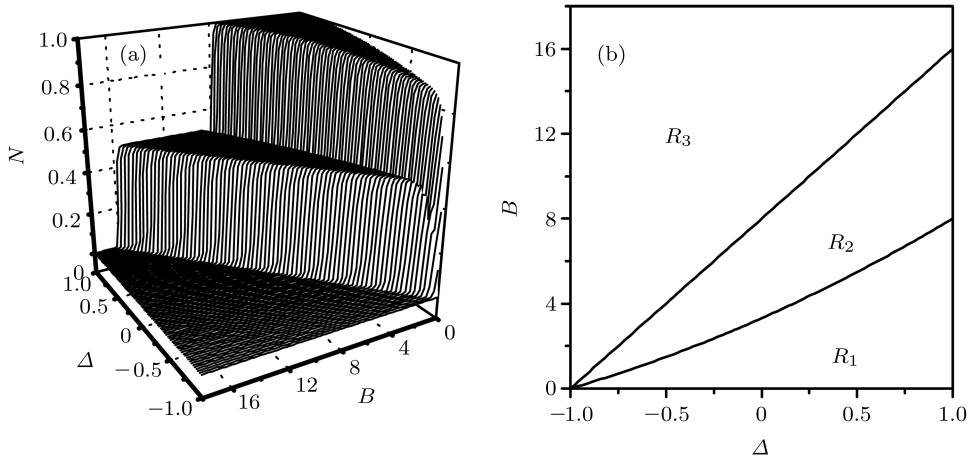



**Fig.1.** The ground-state entanglement and transitions.(a) The ground-state entanglement for $L = 2, J = 4$ versus magnetic field $B$ and anisotropy $\Delta$. (b) The ground state transitions shown by three regions in the plane of $B$ and $\Delta$.

The effects of the anisotropic coefficient $\Delta$ and magnetic field $B$ on the negativity $N$ are clearly shown in Fig.1. From Fig.1(a), it is seen that the ground-state entanglement will experience two kinds of transitions with the increase of $B$ for a certain value of $\Delta$. This unique property can be explained by the change of the ground state $|\psi\rangle_{\text{ground}}$. According to Eq.(4), $|\psi\rangle_{\text{ground}}$ can change from $|\psi_8\rangle$ to $|\psi_5\rangle$, then to $|\psi_9\rangle$ when $B$ is increased from zero. For the antiferromagnetic case of $J > 0$, the transitions of $|\psi\rangle_{\text{ground}}$ are given by

$$|\psi\rangle_{\text{ground}} = \begin{cases} |\psi_8\rangle, & 0 \le B < -2J + J(\Delta + \sqrt{\Delta^2+8}), \\ |\psi_5\rangle, & -2J + J(\Delta + \sqrt{\Delta^2+8}) \le B < 2J(1+\Delta), \\ |\psi_9\rangle, & B \ge 2J(1+\Delta). \end{cases} \tag{5}$$

In Fig.1(b), the transitions of the ground state are illustrated in the parameter plane of $B$ and $\Delta$. In the region $R_1$, the ground state is $|\psi_8\rangle$ where the maximal entanglement is obtained. In the region $R_2$, $|\psi_5\rangle$ is the ground state and it is still entangled. There is always no entanglement when the parameters are in the region $R_3$ for the ground state is a separable (unentangled) state of $|\psi_9\rangle$. It is clearly seen that the transitions of the ground state are closely dependent on the anisotropy $\Delta$ and magnetic field $B$.

## 3. Entanglement at any finite temperature

Due to the unavoidable effect of thermal temperature, it is necessary to study the entanglement at any finite temperature in a Heisenberg spin-1 chain. The general thermal state at an equilibrium temperature $T$ can be expanded by the eigenvalues $E_i$ and eigenstates $|\psi_i\rangle$ as follows:

$$\rho(T) = \frac{1}{Z}\sum_{i=1}^{3^L} \exp(-E_i/T)|\psi_i\rangle\langle\psi_i|, \tag{6}$$

where $Z$ is the partition function and is given by $Z = \sum_i \exp(-E_i/T)$. Similarly, the case of $L = 2$ is considered. According to the analytical results of $E_i$ and $|\psi_i\rangle$ for two spins in Eq.(4), the thermal equilibrium state $\rho$ can

be easily obtained. To quantitate the thermal entanglement, the partial transpose of $\rho$ can be derived in the space $H$ and expressed as

$$\rho^{T_1} = \frac{1}{Z}\begin{pmatrix} A_1 & 0 & 0 & 0 & A_2 & 0 & 0 & 0 & A_3 \\ 0 & A_4 & 0 & 0 & 0 & A_5 & 0 & 0 & 0 \\ 0 & 0 & A_6 & 0 & 0 & 0 & 0 & 0 & 0 \\ 0 & 0 & 0 & A_4 & 0 & 0 & 0 & A_7 & 0 \\ A_2 & 0 & 0 & 0 & A_8 & 0 & 0 & 0 & A_9 \\ 0 & A_5 & 0 & 0 & 0 & A_{10} & 0 & 0 & 0 \\ 0 & 0 & 0 & 0 & 0 & 0 & A_6 & 0 & 0 \\ 0 & 0 & 0 & A_7 & 0 & 0 & 0 & A_{10} & 0 \\ A_3 & 0 & 0 & 0 & A_9 & 0 & 0 & 0 & A_{11} \end{pmatrix}, \tag{7}$$

where the parameters $A_i$ are given by

$$\begin{aligned} A_1 &= \mathrm{e}^{-\frac{2B+2J\Delta}{T}}, \quad A_2 = \frac{1}{2}\mathrm{e}^{-\frac{2J+B}{T}} - \frac{1}{2}\mathrm{e}^{-\frac{-2J+B}{T}}, \\ A_3 &= -\frac{1}{2}\mathrm{e}^{\frac{2J\Delta}{T}} + a_+^2\mathrm{e}^{-\frac{4JX_+}{T}} + a_-^2\mathrm{e}^{-\frac{4JX_-}{T}}, \quad A_4 = \frac{1}{2}\mathrm{e}^{-\frac{2J+B}{T}} + \frac{1}{2}\mathrm{e}^{-\frac{-2J+B}{T}}, \\ A_5 &= a_+b_+\mathrm{e}^{-\frac{4JX_+}{T}} + a_-b_-\mathrm{e}^{-\frac{4JX_-}{T}}, \quad A_6 = \frac{1}{2}\mathrm{e}^{\frac{2J\Delta}{T}} + a_+^2\mathrm{e}^{-\frac{4JX_+}{T}} + a_-^2\mathrm{e}^{-\frac{4JX_-}{T}}, \\ A_7 &= a_+b_+\mathrm{e}^{-\frac{4JX_+}{T}} + a_-b_-\mathrm{e}^{-\frac{4JX_-}{T}}, \quad A_8 = b_+^2\mathrm{e}^{-\frac{4JX_+}{T}} + b_-^2\mathrm{e}^{-\frac{4JX_-}{T}}, \\ A_9 &= \frac{1}{2}\mathrm{e}^{-\frac{2J+B}{T}} - \frac{1}{2}\mathrm{e}^{\frac{2J+B}{T}}, \quad A_{10} = \frac{1}{2}\mathrm{e}^{-\frac{2J-B}{T}} + \frac{1}{2}\mathrm{e}^{\frac{2J+B}{T}}, \quad A_{11} = \mathrm{e}^{-\frac{-2B+2J\Delta}{T}}. \end{aligned} \tag{8}$$

In the above equations, $X_\pm, a_\pm$, and $b_\pm$ are the same as those in Eq.(4).

The dependence of negativity $N$ on temperature $T$ and anisotropy $\Delta$ is plotted in Fig.2. It is seen that the entanglement always decreases as temperature $T$ increases and finally vanishes at a certain temperature. The temperature at which the negativity $N$ vanishes increases as the anisotropy $\Delta$ increases. In Fig.2(a), the negativity $N$ is plotted as a function of $T$ and $\Delta$ when $B = 5 < 2J$. For low temperatures, there are two peaks in $N$, whose values are about 0.5 and 1.0, located at about $\Delta \approx -0.3 - 0.3$ and $0.4 - 1.0$ respectively. The ground state may change from $|\psi_8\rangle$ to $|\psi_5\rangle$, and then to $|\psi_9\rangle$.

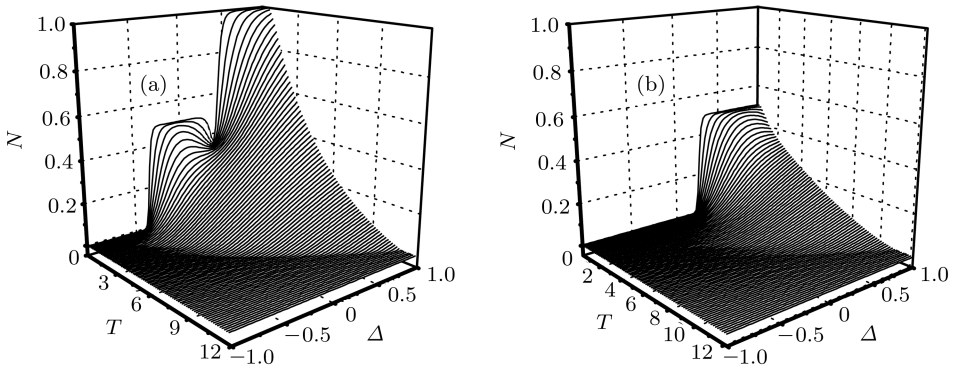



**Fig.2.** The thermal entanglement $N$ for $L = 2, J = 4$ versus temperature $T$ and anisotropy $\Delta$ when the magnetic field is varied from (a) $B = 5 < 2J$ to (b) $B = 10 > 2J$.

After the mixture of other unentangled components, the thermal entanglement will decline. Therefore, the entanglement decreases from two different peaks separately. In Fig.2(b), the $N$ is plotted as a function of $T$ and $\Delta$ when $B = 10 > 2J$. For low temperatures, there is only one peak in $N$, whose value is about 0.5, located at about $\Delta \approx 0.25 - 1.0$. The ground state only changes from $|\psi_5\rangle$ to $|\psi_9\rangle$. When the amplitude of magnetic field $B$ is varied, the relations between $N$ and $\Delta$ are quite different, which is clearly shown in Figs.2(a) and 2(b). This is the reason why the ground state changes for the different values of magnetic field $B$.

If the spin number $L > 2$, the negativity $N$ can be obtained only numerically. Through the numerical calculations under periodic boundary condition, the values of negativity $N$ of the nearest and the next-nearest spins against magnetic field strength $B$ for several values of anisotropy in Fig.3. The $N$ of the nearest spin is plotted as a function of $B$ in Fig.3(a), with $\Delta$ take as a variable parameter. From Fig.3(a), it is seen that the entanglement between the nearest spins increases as the anisotropy $\Delta$ increases but decreases as the magnetic field $B$ increases. For $\Delta > 0$, the nearest-neighbour entanglement $N_{i,i+1}$ is always dominant in the entanglement between any two spins. The negativity $N$ of the next-nearest spins is plotted as a function of $B$ in Fig.3(b), with $\Delta$ taken as a variable parameter. From Fig.3(b), it is seen that there is a peak in $N$. The location of the peak shifts to large values of $B$ as $\Delta$ increases. The height of the peak decreases as $\Delta$ increases. When the anisotropy $\Delta < 0$, the maximum peak appears in the next-nearest-neighbour entanglement $N_{i,i+2}$. From Fig.3, it is seen that the value of $N_{i,i+1}$ gradually decreases to zero as $B$ increases. When the anisotropy $\Delta$ increases, $N_{i,i+1}$ is enhanced. While the value of $N_{i,i+2}$ can arrive at a maximum when $B$ increases to a certain value with a suitable anisotropy $\Delta$. When $\Delta$ increases nearly to 0.3, two peaks with different values may occur in $N_{i,i+2}$. When $\Delta$ is approximately smaller than $-0.4$, the monotonically descending of $N_{i,i+2}$ may occur. It is clear that the entanglement $N_{i,j}$ between the $i$th and the $j$th spins decreases rapidly when the separation $|j-i|$ between the spins increases.

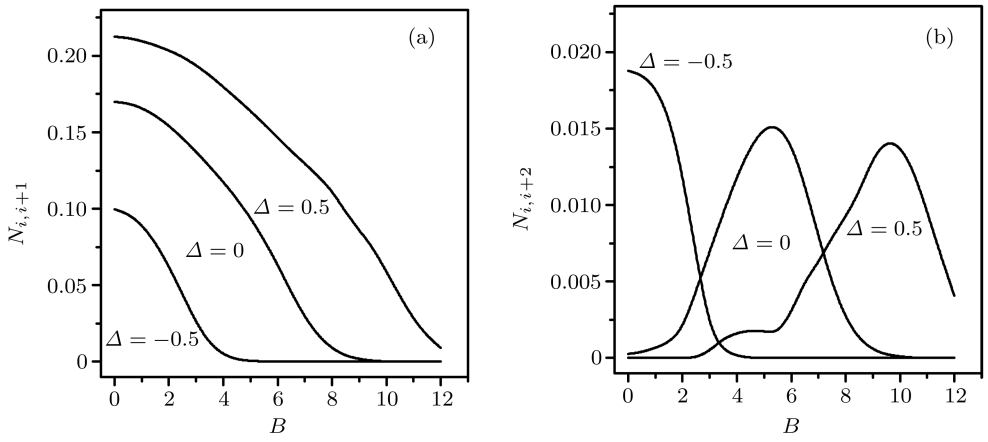



**Fig.3.** The negativity of many-spin chains for $L = 6, J = 4$ versus magnetic field $B$ for the different values of anisotropy $\Delta$. (a) The nearest-neighbour entanglement $N_{i,i+1}$ and (b) the next-nearest-neighbour entanglement $N_{i,i+2}$.

## 4. Effects of boundary condition and system size

In a strongly correlated quantum spin system, the entanglement properties are closely related to the boundary condition and the system size.[38−40] It is necessary to investigate the effects of boundary condition on the entanglement when the spin system size $L$ increases. For the spin-1 Heisenberg model, there are two kinds of boundary conditions. One is the periodic boundary condition (PBC) and the other is the open boundary condition (OBC). Under these two kinds of boundary conditions, the quantum state of the isotropic spin-1 Heisenberg chain is always SU(2) invariant.[41] Therefore, the entanglement at any state between the nearest-neighbour spins can be obtained regardless of the boundary condition

$$N_{i,i+1} = \max\left\{\frac{\langle(\boldsymbol{S}_i \cdot \boldsymbol{S}_{i+1})^2\rangle}{2} - 1, 0\right\}. \qquad (9)$$

For the ground state of large finite system size $L$, the correlation functions are dependent on different kind of boundary condition. Thus, the entanglement $N_{i,i+1}$ with the OBC is different from that with the PBC.

Using numerical calculations, the entanglements versus system size and versus spin site for two kinds of boundary conditions are plotted in Fig.4 separately. The entanglement $N_{1,2}$ versus system size $L$ for the two different boundary conditions is plotted in Fig.4(a).

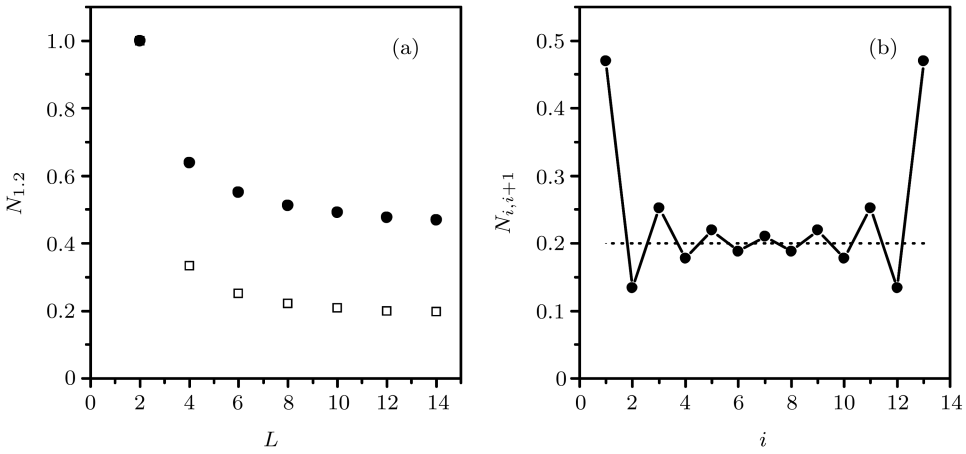



**Fig.4.** The entanglements versus system size and versus spin site separately. (a) The entanglement $N_{1,2}$ at the ground state for $\Delta = 1, J = 4$ versus system size for two kinds of boundary conditions. The solid circle denotes the $N_{1,2}$ with the OBC and the open square denotes that with the PBC. (b) Under the OBC, the nearest-neighbour entanglement $N_{i,i+1}$ versus spin site $i$. The dash line denotes the constant value $N_c \approx 0.2$ of PBC. The solid circle represents the $N_{i,i+1}$ with $L = 14$.

It is clearly seen that the entanglement always decreases and approaches to a constant value $N_c$ as system size $L$ increases. That is, the entanglement can exist in an experimental system with large finite size $L$. From Fig.4(a), it is seen that the entanglement with the OBC is the same as that with the PBC for $L = 2$. While for a very large system size $L$, the entanglement with the OBC is much larger than that with the PBC. This is consistent with the previous analysis.[24,39,40] If the system size $L$ is very large, the asymptotic value of the correlation function at the ground state can be calculated. When the system size is $L \to \infty$, the values of $\langle(\boldsymbol{S}_1 \cdot \boldsymbol{S}_2)^2\rangle_{L\to\infty} \approx 2.4$ for the periodic boundary condition (PBC) and 2.9 for the open boundary condition (OBC). According to Eq.(9), the entanglement $N_{1,2}(L \to \infty) \approx 0.2$ (PBC) and 0.45 (OBC). Therefore, the constant value $N_c$ varies for different boundary conditions. The nearest-neighbour entanglement $N_{i,i+1}$ as a function of the spin site $i$ is plotted in Fig.4(b) when the system size is $L = 14$. The entanglement $N_{i,i+1}$ with the open boundary condition is represented by the solid circles and the zigzag line. While the entanglement $N_{i,i+1}$ with the periodic boundary condition is shown by the dotted horizontal line. For the open boundary condition, it is seen that the value of $N_{i,i+1}$ is symmetric about the middle site $\frac{L}{2}$. The values of the entanglement $N_{1,2} = N_{L-1,L}$ at the two ends of the spin-1 chain are maxima. Then the value of $N_{i,i+1}$ oscillates and approaches to $N_c$ at $\frac{L}{2}$ when the spin site $i$ increases. When the system size $L$ becomes very large ($L \geq 14$), the value of the entanglement with the OBC at the middle site $i = \frac{L}{2}$ is very close to that with the PBC. This is due to the fact that the interaction environment between the sites $\frac{L}{2} - 1$ and $\frac{L}{2}$ or $\frac{L}{2}$ and $\frac{L}{2} + 1$ with the OBC is almost the same as that with the PBC between two nearest-neighbour sites when the system size $L$ is very large. That is, there is almost no influence of the OBC on the entanglement $N_{i,i+1}$ at the middle site of the spin-1 chain for very large $L$.

## 5. Discussion

The negativity $N$ is used to investigate the entanglement of an anisotropic spin-1 Heisenberg chain in a uniform magnetic field $B$. For the simplest case of $L = 2$, the ground state experiences two kinds of transitions when the field $B$ and the anisotropy $\Delta$ are varied. At a finite temperature, the entanglement decreases and then disappears as the temperature increases. If $B > 2J$, there is one peak in $N$ with a maximum value of $N = 0.5$. If $B < 2J$, there are two peaks with maximum values of $N = 1.0$ and 0.5 for the different values of anisotropic coefficient $\Delta$. For a many-spin chain of $L > 2$, the entanglement decreases rapidly as the separation $|j - i|$ between spins increases. Compared with the entanglement of the nearest-neighbour spins, there is a peak in the entanglement of the next-nearest-neighbour spins and the peak increases when the anisotropy $\Delta < 0$. The next-nearest-neighbour entanglement can be improved when the magnetic field $B$ increases to a certain value.

The entanglement $N_{1,2}$ always decreases and approaches to constant values of $N_c$ as the spin number $L$ increases regardless of the boundary conditions. The constant value $N_c$ with the OBC is much larger than that with the periodic boundary condition. For the open boundary condition of very large system size $L$, the nearest-neighbour entanglement $N_{\frac{L}{2}-1,\frac{L}{2}}$ or $N_{\frac{L}{2},\frac{L}{2}+1}$ at the middle site of the spin chain is almost the same as that with the periodic boundary condition. For a very large system size $L$, the effect of the OBC on the middle site of the spin chain is extremely weak. Near the middle site, the entanglement between the two spins is similar to that with the PBC.

From the results shown in Figs. 1 and 2, it is interesting to note that the entanglement between two spins can jump from zero to 0.5 and then to 1.0 by varying the external magnetic field $B$, the temperature $T$, and the anisotropy $\Delta$ of the system. This property may be used to construct two different kinds of entanglement switches. One kind of switch may control the entanglement change from 0 to 0.5, and the other may vary the entanglement from 0.5 to 1.0. In solid-state quantum information processing, this entanglement switch may be used to select and keep some useful quantum states. The Heisenberg spin systems may be used in information storage and logic gate operation in quantum computation. Recently, in polycrystalline NiFe magnetic elements of nanometre-scale magnetic quantum-dot cellular automata systems, the nanomagnets have been arranged in either ferromagnetically or antiferromagnetically ordered state. The logic gate operation could be performed in such spin-based systems.[42] Meanwhile, the collective spin configuration and the strength of the coupling between the atomic spins in the atomic-scale magnetic linear chains of 1-to-10 manganese atoms have been measured and analysed by the Heisenberg model for open chain of $N$ coupled spins.[43]

## Acknowledgment

It is a pleasure to thank Ren Jie for his help with numerical calculations.

## References

[1] Einstein A, Podolsky B and Rosen N 1935 *Phys. Rev.* **47** 777
[2] Schrodinger E 1935 *Naturwissenschaften* **23** 807
[3] Bennett C H and DiVincenzo D P 2000 *Nature* **407** 247
[4] Feng M, D'Amico I, Zanardi P and Rossi F 2003 *Phys. Rev.* A **67** 0414306
[5] Gasparoni S, Pan J W, Walther P, Rudolph T and Zeilinger A 2004 *Phys. Rev. Lett.* **93** 020504
[6] Liu J M, Li J and Guo G C 2002 *Chin. Phys.* **11** 339
[7] O'Connor K M and Wootters W K 2001 *Phys. Rev.* A **63** 052302
[8] Cao M and Zhu S 2005 *Phys. Rev.* A **71** 034311
[9] Liao X P, Fang M F, Zheng X J and Cai J W 2006 *Chin. Phys.* **15** 353
[10] You J, Li J H and Xie X T 2005 *Chin. Phys.* **14** 1329
[11] Hou X W, Hui Z, Ding R M, Chen X Y and Gao Y 2006 *Chin. Phys.* **15** 2510
[12] Xu C T, Chen G, He M M and Liang J Q 2006 *Chin. Phys.* **15** 2828
[13] Shor P W 1996 *Phys. Rev. Lett.* **77** 793
[14] Grover L K 1997 *Phys. Rev. Lett.* **79** 325
[15] Imamoglu A, Awschalom D D, Burkard G, DiVincenzo D P, Loss D, Sherwin M and Small A 1999 *Phys. Rev. Lett.* **83** 4204
[16] Christandl M, Datta N, Ekert A and Landahl A J 2004 *Phys. Rev. Lett.* **92** 187902
[17] Arnesen M C, Bose S and Vedral V 2001 *Phys. Rev. Lett.* **87** 017901
[18] Zhang G F and Li S S 2005 *Phys. Rev.* A **72** 034302
[19] Hao X and Zhu S 2005 *Phys. Lett.* A **338** 175
[20] Skomski R, Istomin A Y, Starace A F and Sellmyer D J 2004 *Phys. Rev.* A **70** 062307
[21] Zhang G F and Li S S 2005 quant-ph 0509014
[22] Wang X G 2001 *Phys. Rev.* A **64** 012313
[23] Tribedi A and Bose I 2006 *Phys. Rev.* A **74** 012314
[24] Wang X G 2004 *Phys. Rev.* E **69** 066118

[25] Osborne T J and Nielsen M A 2002 *Phys. Rev.* A **66** 032110
[26] Dür W, Hartmann L, Lewenstein M and Briegel H J 2005 Phys. *Rev. Lett.* **94** 097203
[27] Gühne O and Tóth G 2005 quant-ph 0510186
[28] Osterloh A, Amico L, Falcl G and Fazlo R 2002 *Nature* **416** 608
[29] Zhou L, Yi X X, Song H and Guo Y 2005 *Chin. Phys.* **14** 1168
[30] Cao M and Zhu S Q 2006 *Chin. Phys. Lett.* **23** 2888
[31] Leidl R and Selke W 2004 *Phys. Rev.* B **69** 056401
[32] Tóth G 2005 *Phys. Rev.* A **71** 010301
[33] Dowling M R, Doherty A C and Barlett S D 2004 *Phys. Rev.* A **70** 062113
[34] Li S S 2005 quant-ph 0510129
[35] Hao X and Zhu S 2005 *Phys. Rev.* A **72** 042306
[36] Verstraete F, Popp M and Cirac J I 2004 *Phys. Rev. Lett.* **92** 027901
[37] Peres A 1996 *Phys. Rev. Lett.* **77** 1413
[38] Verstraete F, Porras D and Cirac J I 2004 *Phys. Rev. Lett.* **93** 227205
[39] Laflorencie N, Sorensen E S, Chang M S and Affleck I 2006 *Phys. Rev. Lett.* **96** 100603
[40] Fan H, Korepin V, V. Roychowdhury, Hadley C and Bose S 2006 quant-ph 0605133
[41] Schliemann J 2003 *Phys. Rev.* A **68** 012309
[42] Imre A, Csaba G, Ji L, Orlov A, Bernstein G H and Porod W 2006 *Science* **311** 205
[43] Hirjibehedin C F, Lutz C P and Heinrich A J 2006 *Science* **312** 1021